Jurnal Mekanikal
Dec 2013, No 36, 66-85

CONTROL OF A SINGLE LINK ROBOT ARM ACTUATED BY PNEUMATIC ARTIFICIAL MUSCLES EMPLOYING ACTIVE FORCE CONTROL AND FUZZY LOGIC VIA HARDWARE-IN-THE-LOOP-SIMULATION

A. Enzevaee*, M. Mailah, S. Kazi

Department of Applied Mechanics and Design
Faculty of Mechanical Engineering
Universiti Teknologi Malaysia
81310 Skudai, Johor Bahru, Malaysia

ABSTRACT

Among the many types of actuation for robotic systems, Pneumatic Artificial Muscle (PAM) is one of the most credible and efficient classes providing high tension forces, high power density, rapid response and high power-to-weight ratio, as well as features like cleanliness and low cost. However, drawbacks such as high level of nonlinearity and time varying characteristics make this class of actuators difficult to control. In this paper, an intelligent Active Force Control(AFC) of a single-link PAM actuated robot arm employing Fuzzy Logic(FL) element has been applied and tested through simulation as well as experimental studies. The robot arm is desired to move along a one radian (about 60 degrees) circular trajectory as a joint angle tracking control in the wake of the introduced disturbances. To demonstrate the robot arm more industrially practical, a radial gripper has been physically developed and attached to the robot arm. The experiment was conducted using Hardware-in-the-Loop-Simulation (HILS) strategy, taking into account variations in the payload masses. The results clearly show the capability of the proposed controller to handle and eliminate the disturbances in the system effectively and robustly.

Key words: *Pneumatic artificial muscle, single link robot arm, active force control, fuzzy logic, hardware-in-the-loop simulation*

1.0 INTRODUCTION

In the recent years, as a result of enormous industrial advancements and the consequent changes in people's lives, human-like robots or humanoids have been given special attention and much time and money is being spent on the careful technical studies on such systems with the purpose of replacing human labor, using in rehabilitation applications, performing accurate repetitive tasks and many more. Robot arms, in this regard, are undoubtedly the most important systems as in many of the applications they are the assets performing the actual tasks. Numerous types of actuators are generally used in the robotic systems, each presenting special performance characteristics. Electrical motor, hydraulic drive and pneumatic drive are among the major ones. For any application based on the system and performance requirements, there are a series of selection criteria for the actuator including high power density, high power-to-weight ratio, accuracy, repeatable control, rapid response, cleanliness, low cost and high efficiency.

The *Pneumatic Artificial Muscle* (PAM) actuator possesses almost all of the mentioned advantages and is therefore considered as one of the best candidate for robotic

*Corresponding author: a_enzevaee@yahoo.com

arm applications. However, due to undesirable characteristics such as inherent nonlinearities, high sensitivity to payload and time-varying performance parameters, force and position control of this class of actuators are challenging. PAM, typically known as McKibben muscle, was invented in the 1950s by the atomic physician Joseph L. McKibben which used the pressure of gas to contract and actuate as a real muscle [1].

PAM generally consists of a flexible rubber tube covered with a cross-weave sheath material and two connection flanges. The contraction force depends on the applied pressure and the muscle's length, ranging from an extremely high value at maximum length (i.e., zero contraction) to zero at minimum length (maximum contraction). Numerous researches have been done on the control of PAM actuated robots. Zhu *et al.* applied a discontinuous projection-based adaptive robust control method to control a three-pneumatic-muscle-driven parallel manipulator through simulation and experimental studies to achieve the precise posture trajectory tracking control [1]. Tondu *et al.* used the principle of virtual work to derive the muscle force model [2]. A similar work was done by Chou and Hannaford to model *McKibben* actuator using the virtual work principle [4]. Repperger *et al.* proposed a typical model in terms of a spring and damper system for pneumatic artificial muscles [3, 4]. Thanh and Ahn proposed the use of neural networks for the tuning of the nonlinear PID controller parameters [5]. Recently, Ahn and Anh developed their work using genetic algorithmto identify the parameters of a 2-link pneumatic artificial muscle manipulator by an ARX model. They also proposed an adaptive recurrent neural network which they implemented for the position control of the joint angle of a two link manipulator actuated by pneumatic artificial muscles [6]. Chan *et al.* carried out a series of simulation studies on the control of pneumatic artificial muscle using fuzzy PD+I for position tracking of the vertical movement of a mass suspended from a pneumatic muscle [7]. Lilly *et al.* implemented an adaptive tracking technique to pneumatic muscle actuators arranged in bicep-tricep configuration [8-10].

A simple, effective and robust control scheme that can be applied for PAM actuated robot control is the *Active Force Control* (AFC) algorithm. Hewit and Burdess were the first researchers who applied AFC in their works and conducted extensive research on the subject [11, 12]. Mailah and fellow researchers extended and consolidated their works by applying the AFC concept to a number of dynamical systems [13-19].

2.0 PNEUMATIC ARTIFICIAL MUSCLES

Artificial muscle actuators were developed for biorobotic systems by Klute [20, 21], and a pneumatic muscle hand therapy device by Koeneman. However, the fluidic muscles (PAM) inherently possess non-linear loading characteristics, hysteresis behaviour, and are susceptible to temperature changes [15, 22, 23]. Also, time variance plus the non-linear behavior of gas, friction, viscosity and etc., which cause disturbances and non-linear functions, make it hard to control the high speed system precisely. Figure 1 illustrates the virtual work principle applied to PAM actuator.

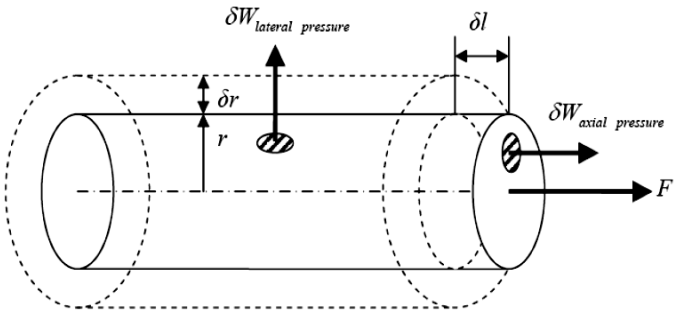

Figure 1: Application of virtual work principle to *McKibben* actuator

From the virtual work theorem, it can be deduced for the PAM:

$$\delta W_{lateralpressure} + \delta W_{axialpressure} + \delta W_{equilibriumforce} = 0 \quad (1)$$

$$(2\pi r l P)(\delta r) - (\pi r^2 P)(-\delta l) - F(-\delta l) = 0 \quad (2)$$

Where r and P denote the radius of the muscle and the internal pressure, respectively.

The expression for the force produced by the PAM can be obtained in terms of a function of control pressure, P and the contraction ratio ε, as follows:

$$F(\varepsilon, P) = (\pi r_0^2) P[a(1 - k\varepsilon)^2 - b] \quad (3)$$

where $= \frac{3}{\tan^2(\alpha_0)}$, $b = \frac{1}{\sin^2(\alpha_0)}$ and $\varepsilon = \frac{l_0 - l}{l_0}$. Also, r_0 is the initial radius of the PAM and α_0 is defined as the angle between the PAM axis and each thread of the braided sheath before expansion.

3.0 KINEMATICS AND DYNAMICS OF THE ROBOT ARM

The general configuration of the robotic system under study is depicted in Figure 2a.

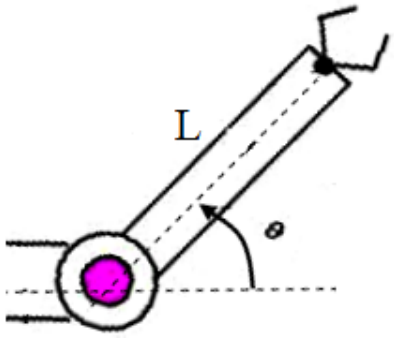

Figure 2a : A representation of the single link robot arm

In this figure, θ is the joint angle and L is the length of the arm. Taking x and y as the *Cartesian* coordinates of the end-effector position, the kinematic model of the robot arm can be written as follows:

$$x = L\cos(\theta) \quad (4)$$

$$y = L\sin(\theta) \quad (5)$$

Applying the inverse kinematics, the joint angle can be expressed as:

$$\theta = \arccos(x) \quad (6)$$

or

$$\theta = \arcsin(y) \quad (7)$$

Lagrange's formulation has been used to derive the equation of motion for the nonlinear dynamic system. The general equation for the dynamics of a rotating manipulator can be described as the torque at the joint:

$$\tau = H(\theta)\ddot{\theta} + h(\theta,\dot{\theta}) + G(\theta) + \tau_d \tag{8}$$

where $H(\theta)$ refers to the inertia of the arm, h accounts for the *Coriolis* and centripetal effects, G represents the gravitational torque and τ_d is the disturbance torques. The robot arm in this study is supposed to move in horizontal plane only and hence, the gravitational effects are neglected. Therefore, the governing equation for the actuator torque for a single link arm is reduced to:

$$\tau = I\ddot{\theta} + \tau_d \tag{9}$$

where I is the robot arm inertia and $\ddot{\theta}$ is the angular acceleration.

3.1 Robot arm actuated by antagonistic PAM actuators

The robot arm is actuated by a pair of PAMs in antagonistic configuration which has been designed to emulate the human arm biceps-triceps anatomy. The two muscles are connected by a timing belt and pulley mechanism for the transmission of actuator force. The differential pressure and the resultant force difference between the agonist and the antagonist produce a clockwise or counter-clockwise torque. To obtain more linear behavior of the PAM both, actuators are initially pressurized at P_0 from which results in an initial contraction ratio, ε_0. When the agonist muscle is inflated with pressure P_1 different from the antagonist muscle pressure P_2, a rotation of angle θ is produced at the joint. The process is illustrated in Figure 2b.

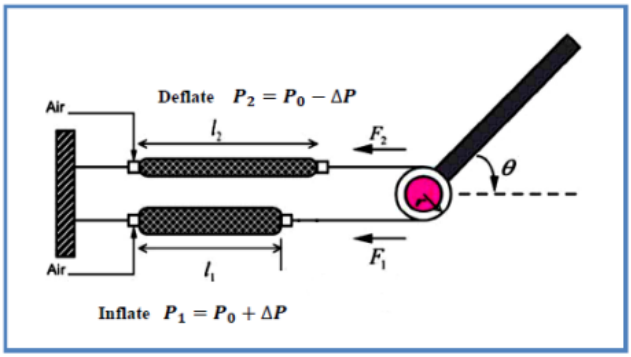

Figure 2b : Antagonistic PAM configuration for a single link robot arm

Denoting the agonist actuator force by F_1 and that of the antagonist by F_2 and the pulley radius by s, the torque produced by the actuator can be formulated as:

$$T = \left(F_1(\varepsilon_1, P_1) - F_2(\varepsilon_2, P_2)\right)s \tag{10}$$

where $\varepsilon_1 = \varepsilon_0 + r\theta/l_0$ and $\varepsilon_2 = \varepsilon_0 - r\theta/l_0$

Considering a monovariable approach of the PAM actuator which can be called symmetrical co-contraction by analogy with the neurophysiological terminology, the symmetrical pressure variation is noted as ΔP. This is the pressure difference applied from initial pressure P_0 in both muscles as $P_1 = P_0 + \Delta P$ and $P_2 = P_0 - \Delta P$. Then the actuator torque model will become:

$$T = 2K_1\Delta P - 2K_2P_0\theta \tag{11}$$

where

$$K_1 = (\pi n_0^2)r[a(1 - k\varepsilon_0)^2 - b \tag{12}$$

$$K_2 = (\pi n_0^2)r2a(1 - k\varepsilon_0)kr/l_0 \tag{13}$$

The static relationship between the pressure difference and the corresponding joint angle can then be obtained as:

$$\theta = G\Delta P \tag{14}$$

$$G = \frac{K_1}{K_2} = \frac{l_0[a(1 - k\varepsilon_0)^2 - b]}{2akr(1 - k\varepsilon_0)P_0} \tag{15}$$

where G represents the open-loop gain.

4.0 CONTROL SCHEMES

In this section, the principal components of the proposed control system for the single link robot arm are presented. It is noteworthy that in the main controller design, Active Force Control with Fuzzy Logic (AFCFL) has been implemented and studied to eradicate the negative effects of disturbances. Note that a *Proportional-Integral-Derivative* (PID) control is first designed prior to AFC-based system which is expected to produce good overall system performance.

4.1 PID Control Loop

For the sake of stability in the system, a PID controller is first considered for the position tracking control. However, it is deemed not sufficient to maintain good performance in the presence of disturbance as it is unable to eliminate the negative effects and the system performance typically degrades at the onset of adverse operating conditions. To compensate for this problem, an AFC-based scheme is directly combined in series with the PID controller for its disturbance rejection capability, thereby providing added robustness of the system. The transfer function of the typical PID controller is as follows:

$$G_c = K_P + \frac{K_I}{s} + K_D s \tag{16}$$

where K_P, K_I, and K_D are the proportional, integral and derivative gains, respectively. These are set and tuned by the heuristic method, employing *One-Value-At-a-Time* (OVAT) technique, i.e., each time changing one parameter while the other two are fixed.

The values corresponding to the least track error are selected for the PID controller parameters and these remain unchanged when the AFC-based scheme is implemented.

4.2 Active Force Control

Among the many control schemes feasible in the area of robot control, *Active Force Control* (AFC) stands out as one with great potentials to eliminate the external disturbance effectively and without too much calculation. The first successful implementation of AFC to a robot arm control was done by Hewit and Burdess in 1981. They proposed a practical and robust technique to compensate for the internal and external disturbances of a mechatronics/machinery system by employing an internal force error feedback control based on real-time acceleration and force measurements. The essential mathematical representation of the AFC controller can be written as:

$$\tau_d^* = \tau - IN\ddot{\theta} \tag{17}$$

where *IN* is the estimated inertia of the link. The purpose of the AFC is to lead the system to arobust, steady and precise state by rejecting any known or unknown disturbances. The simplicity of this method in employing measured values of the specified parameters alongside the estimated value of the inertial/mass parameter, gives the users huge benefit of disregarding many complex mathematical computation of the system due to its non-linear characteristics. However, it is often that the AFC cannot solve the motion control of robotic system by itself without incorporating a lower order of control, i.e., position control that is typically located in the outermost loop. Figure 3 shows a schematic of the AFC control scheme applied to a robot arm with a classical PID controller.

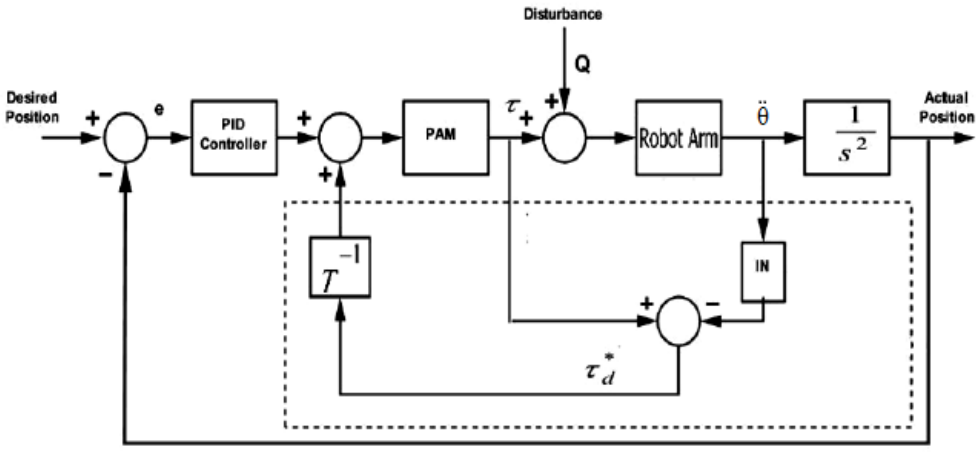

Figure 3 : Schematic of the AFC control scheme

As previously mentioned, the only computational burden in the AFC algorithm is the estimation of the inertia which is to be multiplied by the acceleration of the arm and then compared with the actuator torque to eliminate the undesirable torque caused by the disturbances in the system. Various methods can be used to compute the estimated inertia in the AFC loop such as via intelligent techniques using fuzzy logic (FL), neural networks (NN), iterative learning (IL), etc. In this study, FL is selected and implemented to calculate the robot arm estimated inertia in the AFC section.

4.3 Fuzzy Logic

AFC can perform much more efficiently if a method is used to provide good estimated of the inertia of the arm at any arbitrary moment of time. Thus the proposed AFCFL algorithm exploits the FL as the inertial parameter estimator in the AFC loop. The track error and angular acceleration of the arm are used as inputs to the FL system whereas the estimated inertia of the arm is configured as the output. The proposed scheme is depicted in Figure 4.

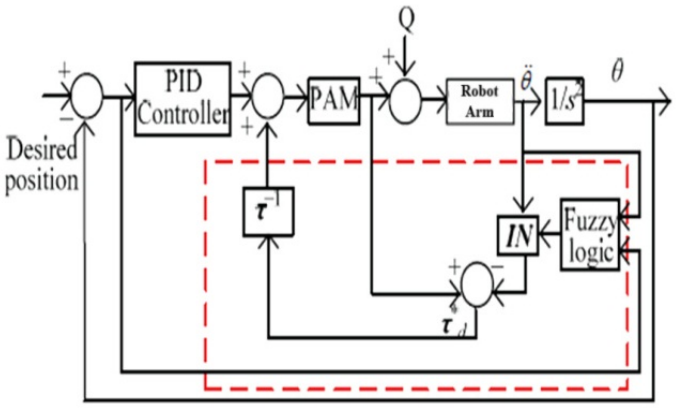

Figure 4 : Schematic of the proposed AFCFL controller

For the simplicity of computation, triangular membership functions for fuzzy sets have been utilized as are tabulated in Tables 1(a) to 1(c) and illustrated in Figures 5(a) to 5(c).

Table 1(a) : Membership functions for the track error

Linguistic Variable: Track error (rad)	
Linguistic Value	Numerical Range
NL	-0.0015 to -0.0005
NS	-0.0001 to 0
Z	-0.0005 to 0.0005
PS	0 to 0.0001
PL	0.0005 to 0.0015

NL: negative large; NS: negative small; Z: zero; PS: positive small; PL: positive large

Table 1(b) : Membership functions for the angular acceleration

Linguistic Variable: Acceleration (rad/s^2)	
Linguistic Value	Numerical Range
NL	-2.25 to -0.75
NS	-1.5 to 0
Z	-0.75 to 0.75
PS	0 to 1.5
PL	0.75 to 2.25

Table 1(c) : Membership functions for the inertia

Linguistic Variable: Inertia (kgm^2)	
Linguistic Value	Numerical Range
VS	-0.1375 to 0.1625
S	0.05 to 0.275
M	0.1625 to 0.3875
B	0.275 to 0.5
VB	0.3875 to 0.6125

VS: very small; S: small; M: medium; B: big; VB: very big

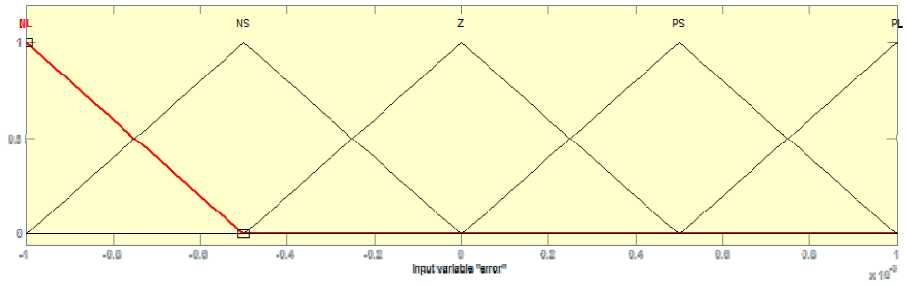

Figure 5(a): Membership functions of the track error (rad)

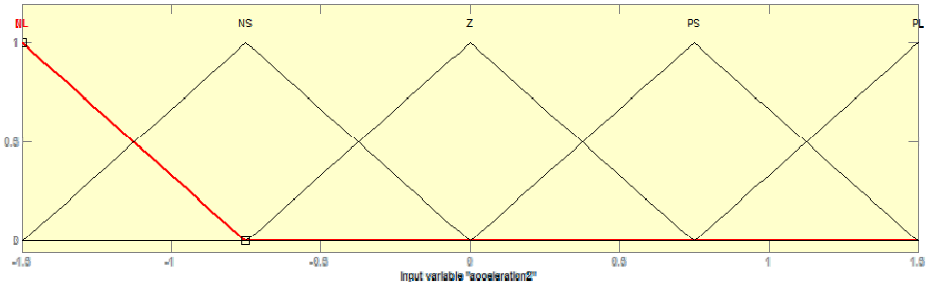

Figure 5(b): Membership functions of the angular acceleration (rad/s^2)

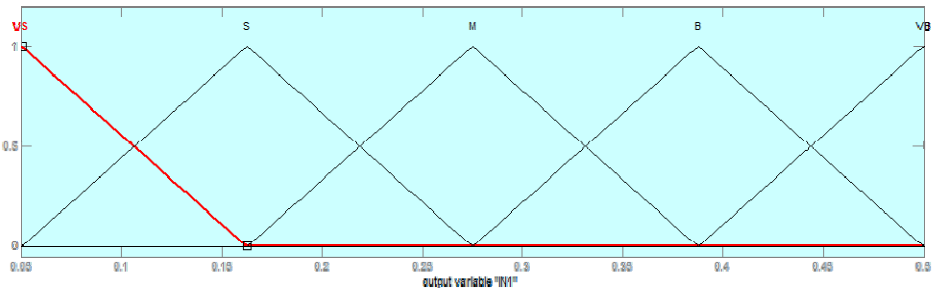

Figure 5(c): Membership functions of the inertia (kgm^2)

The fuzzy rules have been defined and implemented based on the previous works on the same project [13, 15]. The rules are defined in a logical manner as follows:

1. If Trackerror is NL and Acceleration is NL Then IN is VB
2. If Trackerror is NL and Acceleration is NS Then IN is VB
3. If Trackerror is NL and Acceleration is Z Then IN is VB
4. If Trackerror is NL and Acceleration is PS Then IN is B
5. If Trackerror is NL and Acceleration is PL Then IN is M
•
•
•
25. If Trackerror is PL and Acceleration is PL Then IN is M

Table 2 presents the defined fuzzy rules between the inputs and the output of the inertial parameter estimator. It should be noted that the MATLAB *Fuzzy Logic Toolbox* has been used to define the membership functions and fuzzy rules.

Table 2: Fuzzy rules

Estimated Inertia (kgm^2)		**Angular Acceleration (rad/s^2)**				
		NL	NS	Z	PS	PL
Track error(rad)	NL	VB	VB	VB	B	M
	NS	VB	VB	B	M	S
	Z	VB	B	M	S	VS
	PS	B	M	S	VS	VS
	PL	M	S	VS	VS	VS

Finally, a crisp output is obtained through a defuzzification process using an average technique called *centroid* or *center of gravity method* that is proposed in the toolbox as a defuzzification tool and is described by the equation:

$$\bar{x} = \frac{\int \mu_x(x).x\,dx}{\int \mu_x(x)\,dx} \tag{18}$$

5.0 DEVELOPMENT OF GRIPPER

To enhance the PAM robot system and to make it more industrially practical, a 5-member radial gripper was developed, fabricated and integrated into the robot arm for a simple pick-and-place task. Initially, the 3D modeling was done using *Solidworks* software. The parts were then fabricated from aluminium and eventually assembled and attached to the robot arm replacing the previous end-effector. It was attempted to design the gripper in a manner that its weight does not exceed that of the previous end-effector. The 3D sketch of the gripper is illustrated in Figure 6.

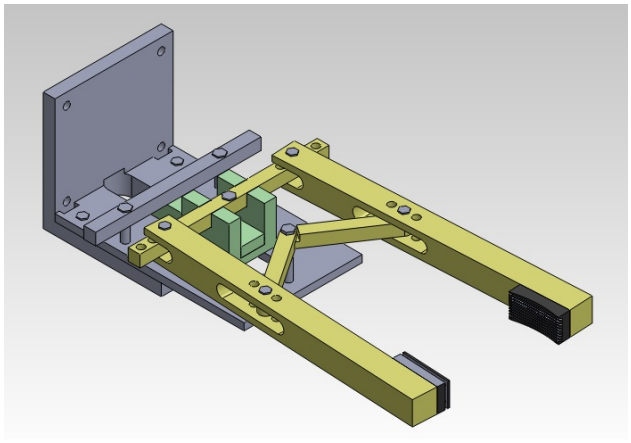

Figure 6: A 3D sketch of the gripper

It was presumed that the gripper is supposed to move and handle objects of maximum load of 150 g and the servo motor driver was intended to be used as the gripper actuator. From static force analysis, an amount of 3.34 N was calculated for the required force provided by the servo motor. Using a rack-and-pinion power transmission unit with 16mm pitch diameter, the calculated actuator torque was obtained as 0.3 kgcm. A DC servo motor (model C55R) was selected as it was available in the market and is able to provide the required torque.

6.0 SIMULATION

Simulation study was carried out using MATLAB/Simulink software. The dynamic model of the robot arm was created in Simulink and the simulation parameters were set as presented in Table 3. The PID controller parameters were finally tuned and set as K_P=250, K_I=40 and K_D=8.

Table 3: Simulation parameters

Structure parameter	Value (SI unit)
Mass of the arm	0.75 kg
Length of the arm	0.34 m
Length of PAM	0.10 m
Diameter of PAM	0.01 m
Diameter of sprocket	0.03 m
Initial pressure	4 bar
Simulation time	10 s
Sampling time	0.01s

In order to investigate the robustness of the proposed controller, a harmonic disturbance torque is assumed on each joint expressed as $Q = 10\sin(40t)$. Figure 7 depicts the Simulink model for the proposed robot control system incorporating AFCFL algorithm.

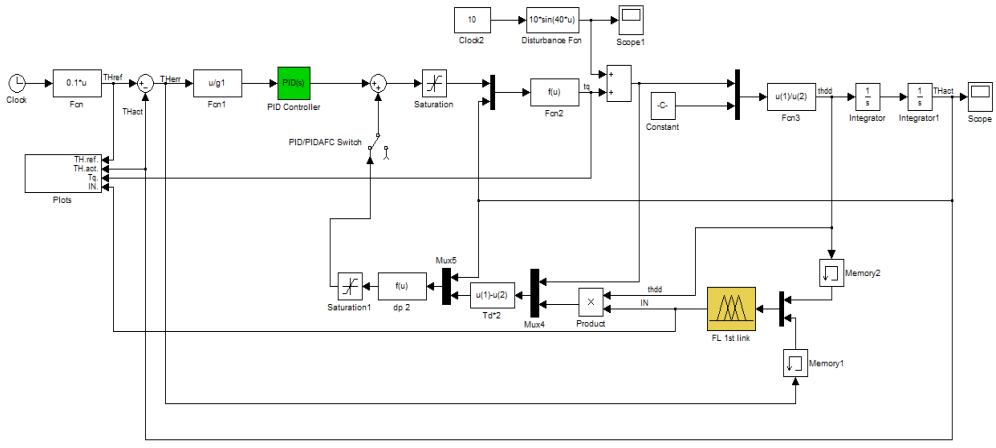

Figure 7: Simulink model for the proposed AFCFL controller

For the servo motor drive, the required input signal was generated through *Pulse Code Modulation* (PCM) in the simulated model which is depicted in Figure 8.

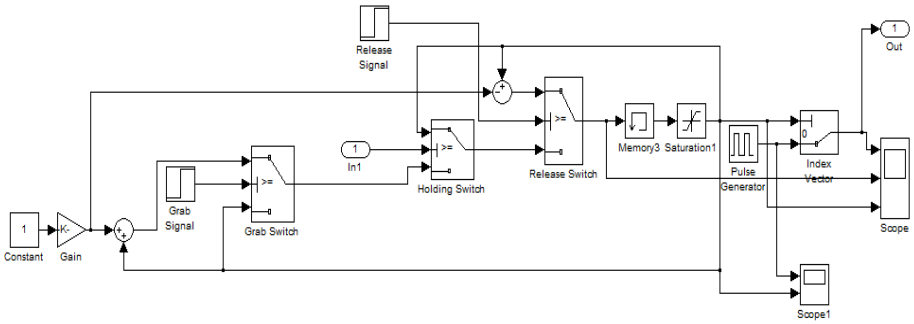

Figure 8 : A Simulink model of the servo PCM pulse generator

7.0 EXPERIMENTATION

The practical feature of the proposed control strategy is presented in this section. Figure 9 presents a view of the mechanical rig and the attached gripper. For the *Hardware-in-the-Loop Simulation* (HILS), a data acquisition card (DAQ) employing the PCI-1710HG model from *Advantech* has been used which collects the analog data from the rotary encoder and through *Analog-to-Digital* (A/D) conversion sends them to the personal computer (PC) to be processed. Implementing MATLAB *Real Time Workshop* (RTW) feature and Simulink, the mechanical rig is integrated with the control system and the digital control signals are then sent from the PC to the DAQ through the *Digital-to-Analog*(D/A) conversion. A pair of PAM (model: DMSP-10-N-100-RM-CM) manufactured by FESTO were used as the actuators. To control the pressure, proportional pressure regulators were utilized. The advantage of using proportional pressure regulator is that no pressure sensor is required because of its built-in pressure controller. Therefore, the mathematical formulation of the pneumatic flow is not required. Thus, in our case, proportional pressure regulators (FESTO,MPPES-3-1/8-10-010) were utilized to control the pressure inside the PAMs. An *Omron* E6B2-CWZ6C rotary encoder to measure the joint angle and an ADXL 335is used as one of the sensory elements in measuring the acceleration of a robotic arm. Table 4 summarizes the details of the hardware employed in the experimental study which are also illustrated in Figures 9 and 10.

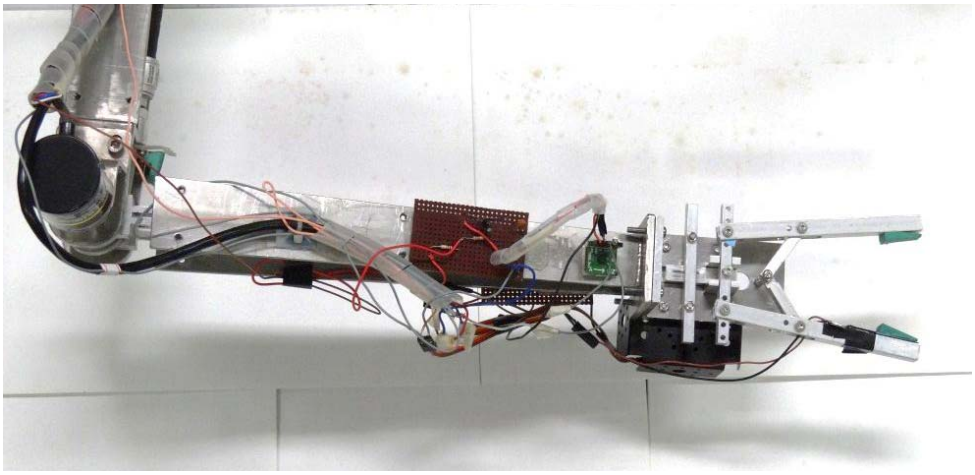

Figure 9 : Top view of the robot arm and the gripper attached

Table 4: Hardware employed in the experimental study

Hardware	Model	Manufacturer	Operating Range
PAM	DMSP-10-N-100-RM-CM	FESTO	0 bar to 8 bar 630 N
Accelerometer	ADXL 335	Analog Devices	±3 g
Rotary encoder	E6B2-CWZ6C	Omron	5V to 24V DC
Proportional pressure regulator	MPPES-3-1/8-10-010	FESTO	0 – 10 bar
Data Acquisition card	PCI-1710HG	Advantech	-10V to 10V 100MHz

PAM | Proportional pressure regulator | Rotary encoder | Accelerometer | DAQ

Figure 10 : Illustration of the main hardware employed in the experimental study

The main experimental study undertaken included the joint angle tracking control of the single-link robot arm under the variation of payload masses. The test objects of the payload masses, m_{pl}=35, 50 and 55 g as well as a 150 g (as the maximum payload mass) were exploited in the experiment. A comparative study was done on the ability of the robot arm to follow the 1 radian prescribed trajectory. The Simulink model with HILS for the experimental study is presented in Figure 11a.

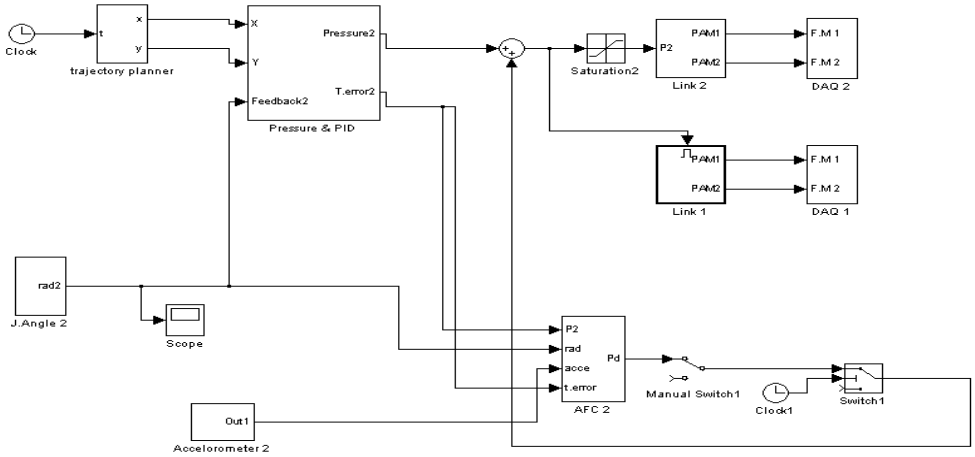

Figure 11a : Simulink model with HILS for the experimental study

8.0 RESULTS AND DISCUSSION

Both simulation and experimental studies were carried out on the single-link robotic arm. The tracking control of robot arm is considered as the basis of the performance criteria to demonstrate the accuracy and effectiveness of the proposed control schemes.

8.1 Simulation results

First, the performance of the simulated model in the absence of the AFC controller was studied. The results showed that the PID controller alone is unable to control and eliminate the disturbance though the performance is stable. However, when the AFCFL controller is applied the effect of the disturbance is eradicated and the robot arm is able to follow the desired trajectory with very small error.

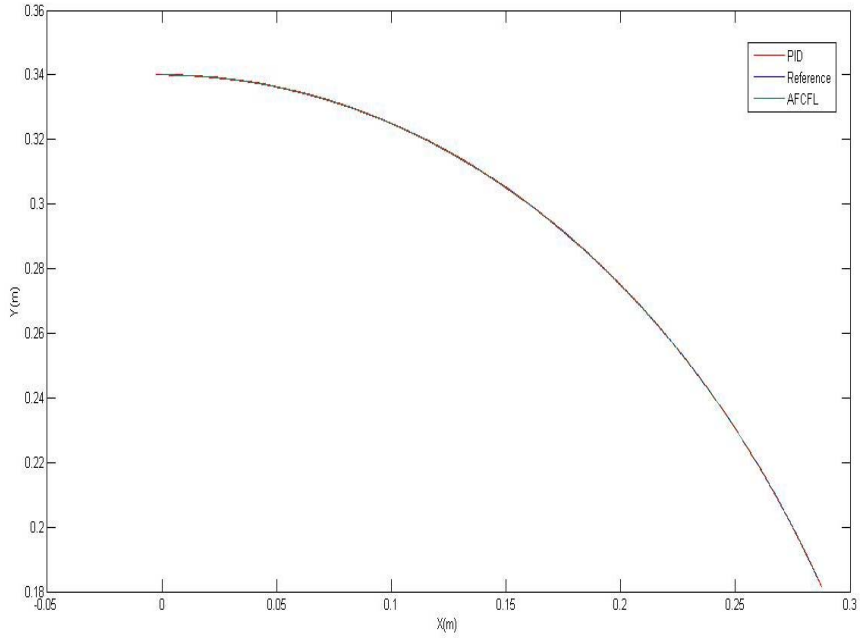

Figure 11b : Trajectory tracking: PID, AFCFL and reference

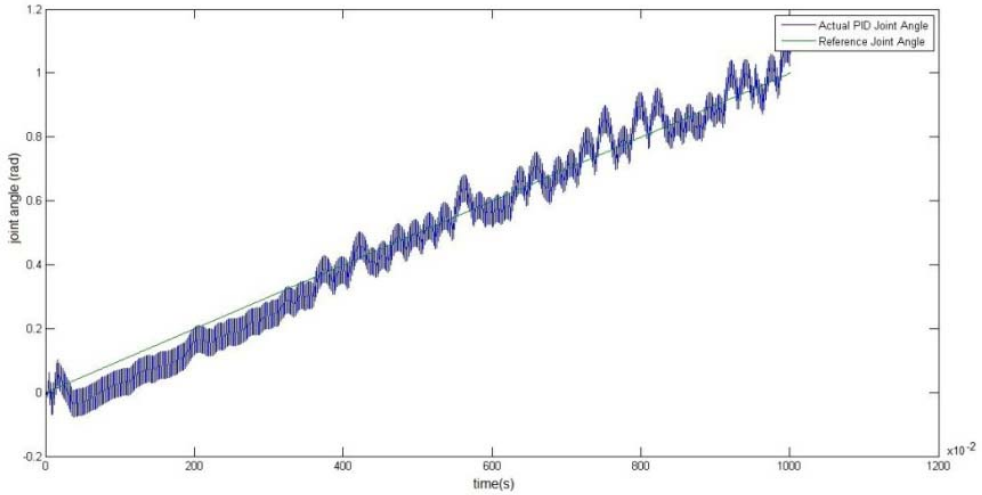

Figure 12 : PID joint angle

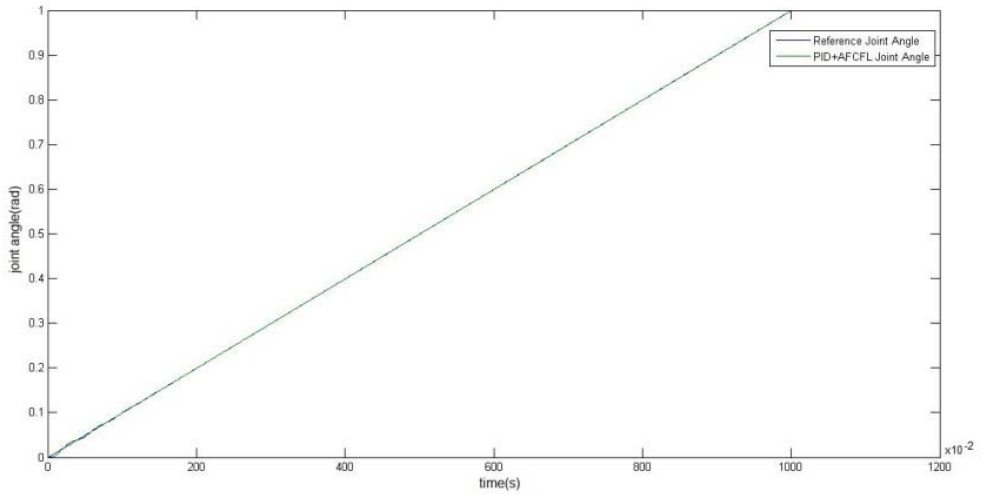

Figure 13: AFCFL joint angle

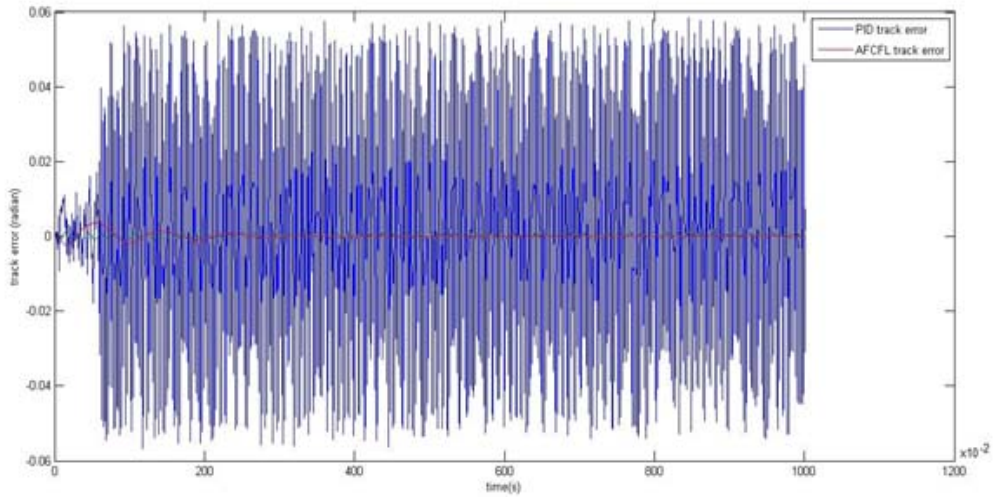

Figure 14: Track error: PID, AFCFL

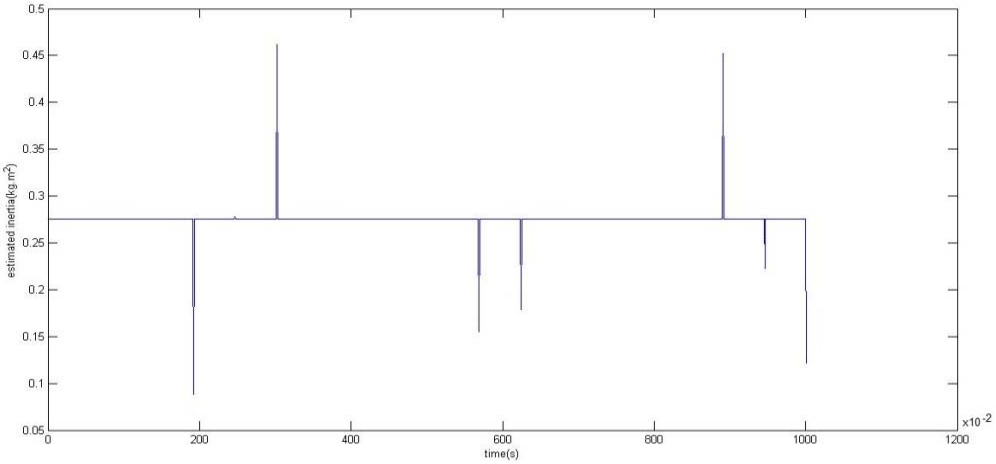

Figure 15 : AFCFL estimated inertia

8.2 Experimental results

Prior to applying the controller, both the PAM actuators were pressurized to 4 bars. Due to the same pressure in each PAM, the torque is zero, hence no motion of the arm. The experiment was carried out four times, considering different payload masses, 30, 50, 55 and 150 g. For each test, the joint angle tracking error was studied. The results show that the system performance is satisfactorily similar to that obtained from the simulation study. Figures 16(a) to (d) present the actual joint angle output of the robot arm for each of the payload masses in the experiment.

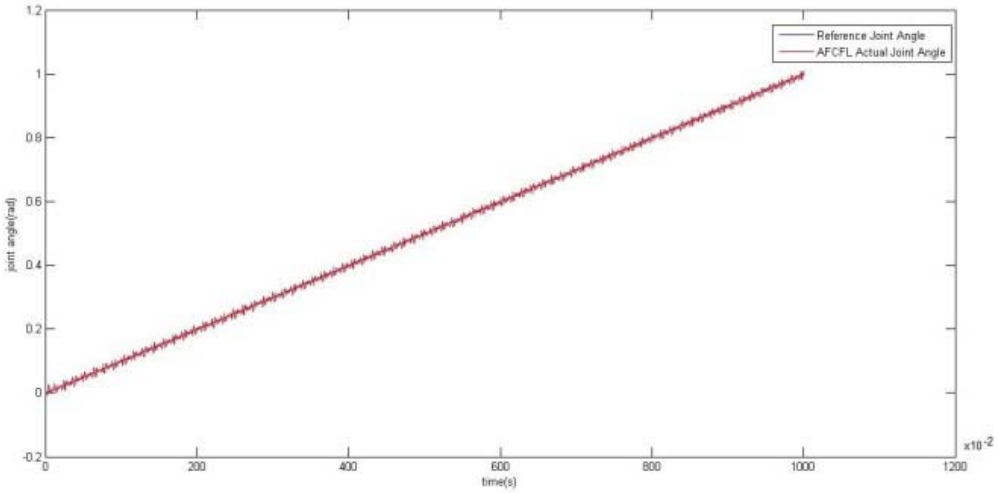

(a)

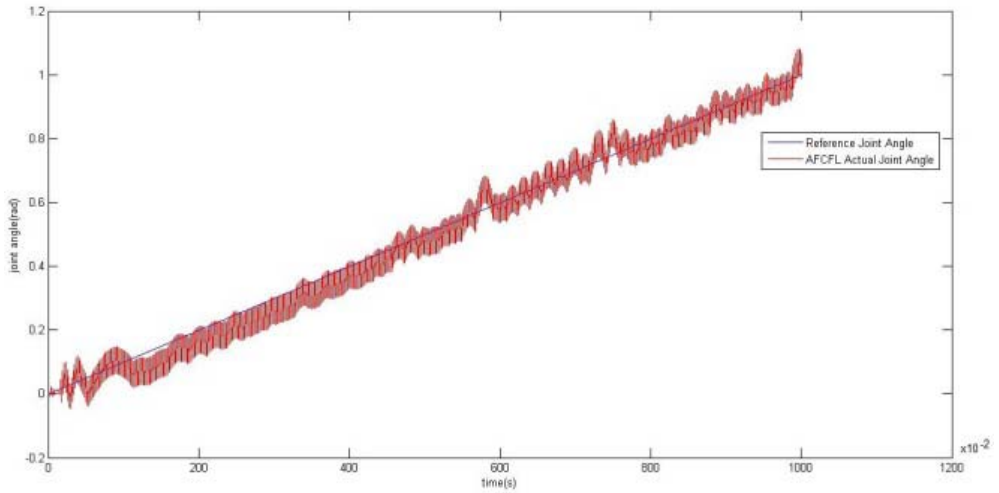

(b)

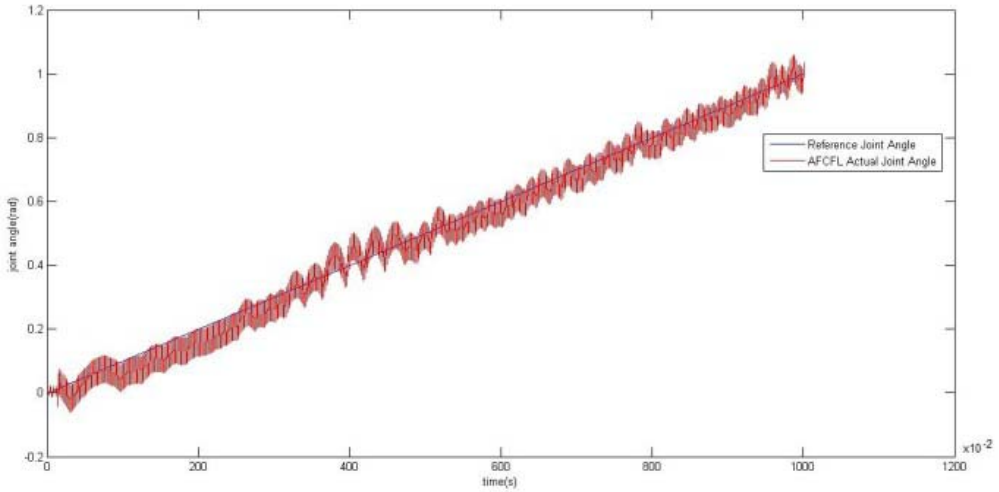

(c)

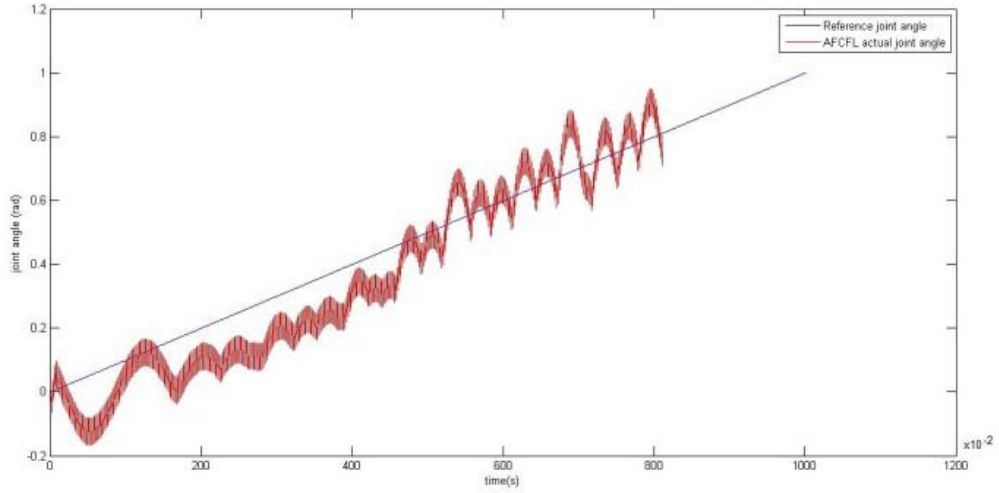

(d)

Figure 16 : Actual joint angle: (a) 30g (b) 50g (c) 55g (d) 150g

Figure 17 (a) to (d) depicts the corresponding track errors. It can be clearly seen that despite the high nonlinear behavior of the PAM actuators, in the presence of AFCFL controller, the robot arm has been able to cope with the negative effect of inherent disturbances in the system. However, as expected, the increase in the payload mass significantly influences the system performance and causes the track error to increase.

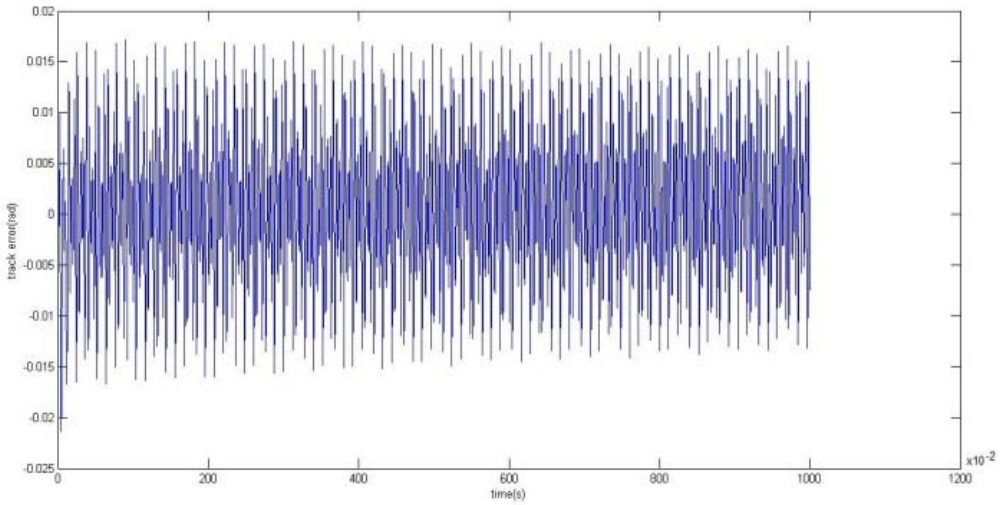
track error(rad)
time(s)
x10^-2

(a)

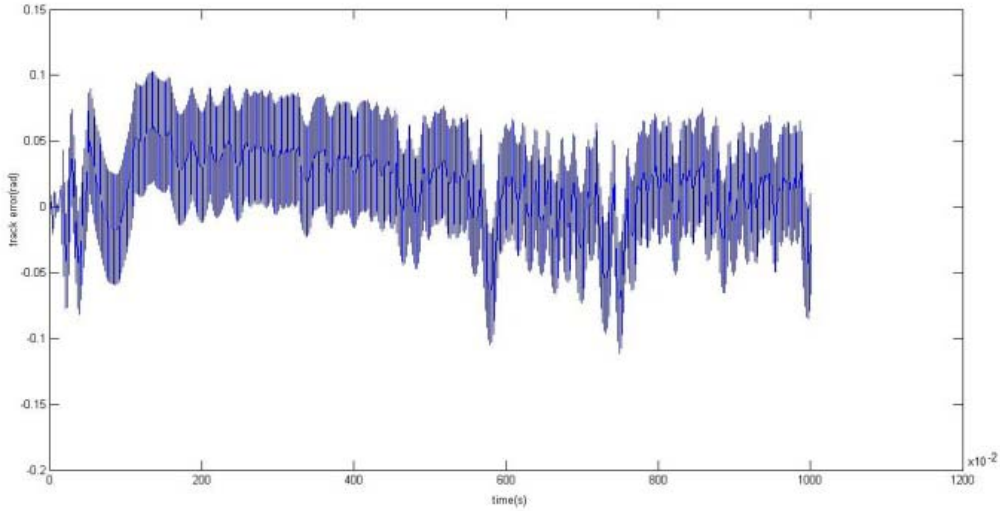
track error(rad)
time(s)
x10^-2

(b)

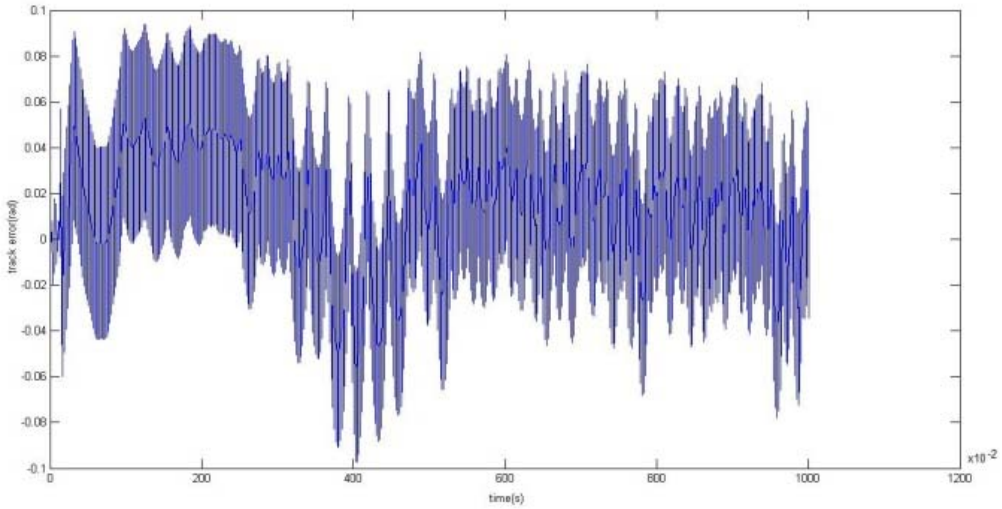
track error(rad)
time(s)
x10^-2

(c)

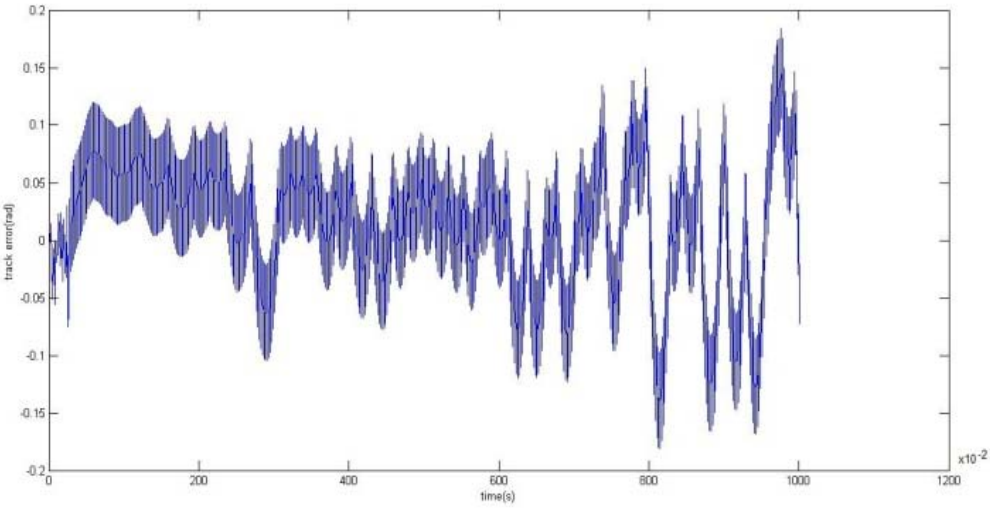

(d)

Figure 17: Actual track error: (a) 30g (b) 50g (c) 55g (d) 150g

In the case of the maximum payload, the robot arm failed to completely follow the prescribed trajectory and stopped at about $\frac{4}{5}$ of the path. This may be mainly due to the fact that PAM actuators are sensitive to the variation in payload masses. It can also be caused by other reasons such as PAM nonlinearity, inconsistent pressure supplied by the air compressor, and noises in the control signals or accelerometer/encoder signals. Nevertheless, the system presents relatively satisfactory performance and the output of the system track error is bound to a limited value. This clearly shows the superiority of the proposed AFCFL.

CONCLUSION

The proposed AFCAFL controller was implemented for the real-time control of a single link planar robotic arm driven by pneumatic artificial muscles. Both the theoretical and practical aspects of the research were carefully investigated.The HILS was successfully applied to integrate the mechanical rig with the control system. The system has been shown to readily operate in real-time. The experimental results verified the theoretical (simulation) counterparts, thereby implying the effectiveness of the proposed algorithm even though the experimental findings exhibit lower levels of accuracy due to a number of physical constraints. The integration of the gripper into the robotic system allowed for studying the performance from a more practical and real life perspective in terms of observing the effect of varying the payload masses. Future works may consider different sets of trajectories as well as the coordinate motion control of a more complex PAM system that will subsequently require more hardware and software integration.

REFERENCES

1. Klute, G.K., Czerniecki, J.M., and Hannaford,B.,1999. McKibben artificial muscles: pneumatic actuators with biomechanical intelligence. *Proceedings of IEEE/ASME International Conference on Advanced Intelligent Mechatronics*.

2. Zhu, X.C., et al., *2008.*Adaptive robust posture control of a parallel manipulator driven by pneumatic muscles*.Automatica, 44(9)*, 2248-2257.
3. Tondu, B. and Lopez,P. 2000. Modeling and control of McKibben artificial muscle robot actuators*.Control Systems, IEEE,. 20(2),*15-38.
4. Chou, C.P. and Hannaford, B., 1996. Measurement and Modeling of McKibbenPneumatic Artificial Muscles, *IEEE Transactions on Robotics and Automation, 12(1),* 90-102.
5. Repperger, D.W., Johnso, K.R. n, and Philips, C.A.,1999.Nonlinear feedback controller design of a pneumatic muscle actuator system. *Proceedings of the American Control Conference, 1999. 1999*.
6. Repperger, D.W., et al., 2005. Power/energy metrics for controller evaluation of actuators similar to biological systems*.Mechatronics*, ***15****(4),* 459-469.
7. Thanh, T.U.D.C. and Ahn,K.K., Nonlinear PID control to improve the control performance of 2 axes pneumatic artificial muscle manipulator using neural network*.Mechatronics*, 2006. 16(9), 577-587.
8. Ahn, K. and Anh,H., 2008. Comparative study of modeling and identification of the pneumatic artificial muscle (PAM) manipulator using recurrent neural networks*.Journal of Mechanical Science and Technology*,*22*(7), 1287-1298.
9. Chan, S.W., et al. 2003. Fuzzy PD+I learning control for a pneumatic muscle. *FUZZ '03. The 12th IEEE International Conference onFuzzy Systems*.
10. Lilly, J.H., 2003. Adaptive tracking for pneumatic muscle actuators in bicep and tricep configurations*.IEEE Transactions onNeural Systems and Rehabilitation Engineering*,. *11*(3), 333-339.
11. Lilly, J.H. and Liang,Y., 2005. Sliding mode tracking for pneumatic muscle actuators in opposing pair configuration*.IEEE Transactions onControl Systems Technology*, 2005. *13(4*), 550-558.
12. Lilly, J.H. and Quesada,P.M., 2004. A two-input sliding-mode controller for a planar arm actuated by four pneumatic muscle groups*.IEEE Transactions onNeural Systems and Rehabilitation Engineering*, *12(3)*, 349-359.
13. Hewit, J.R. and Bouazza-Marouf,K., 1996. Practical control enhancement via mechatronics design*.IEEE Transactions onIndustrial Electronics*,*43(1*),16-22.
14. Hewit, J.R. and J.S. 1981. Burdess, Fast dynamic decoupled control for robotics, using active force control*.Mechanism and Machine Theory*, *16(5*),535-542.
15. Jahanabadi, H., Mailah, M., and Zain, M.Z.M.,*2009*. Active Force Control of a fluidic muscle system using Fuzzy Logic. *IEEE/ASME International Conference onAdvanced Intelligent Mechatronics, AIM*
16. Jahanabadi, H., Mailah, M., and Zain, M.Z.M,2009.Control of a fluidic muscle system using Neuro Active Force Control. *IEEE Symposium onComputational Intelligence in Control and Automation, 2009. CICA*
17. Jahanabadi, H., et al., 2011. Active Force with Fuzzy Logic Control of a Two-Link Arm Driven by Pneumatic Artificial Muscles*.Journal of Bionic Engineering*, *8(4),*474-484.
18. Mailah, M., *Control of a robot arm using iterative learning algorithm with a stopping criterion*, ed. J.W.S. Chong.
19. Mailah, M., 1998. Intelligent active force control of a rigid robot arm using neural network and iterative learning algorithms. *PhD thesis,University of Dundee*.
20. Mailah, M., et al., 2009.Modelling and control of a human-like arm incorporating muscle models*.Proceedings of the Institution of Mechanical Engineers, Part C: Journal of Mechanical Engineering Science*, *223(7),* 1569-1577.
21. Mailah, M. and Rahim, N.I.A.. 2000.Intelligent active force control of a robot arm using fuzzy logic. in *TENCON. Proceedings*.
22. Klute, G.K., 1999. Artificial Muscles: Actuators for Biorobotic Systems.: University of Washington.

23. Klute, G.K., Czerniecki,J.M., and Hannaford, B.,2000. Artificial tendons: biomechanical design properties for prosthetic lower limbs. *Proceedings of the 22nd Annual International Conference of the IEEE*in *Engineering in Medicine and Biology Society,*.
24. Xiaocong, Z., et al., 2008. Adaptive Robust Posture Control of Parallel Manipulator Driven by Pneumatic Muscles With Redundancy*,IEEE/ASME Transactions onMechatronics*, *13(4),*441-450.
25. Reynolds, D.B., et al., 2003. Modeling the Dynamic Characteristics of Pneumatic Muscle*, Annals of Biomedical Engineering*, *31(3),* 310-317.